

Electrochemical characterization of semiconductor photovoltaic silicon

N.Salhi^{1*}, E. Salhi², M.Bounoughaz^{3*}

¹ Laboratory of treatment and forming of polymers, Faculty of Technology,

²National polytechniques school of Algiers

³Department of chemistry Faculty of Sciences

*University of M'Hamed Bougara, Boumerdes 35000, Algeria

*Corresponding author: ne.salhi@univ-boumerdes.dz/ moussa_bounoughaz@yahoo.fr; Tel.: +2130540 17 60 54

ARTICLE INFO

Article History :

Received : 13/01/2020

Accepted : 12/04/2021

Key Words:

electromagnetic crystalline
brewing; defects;
electrochemical techniques;
segregation.

ABSTRACT/RESUME

Abstract: The objective of this search is the use of the electrochemical techniques to verify the homogeneity of the photovoltaic silicon elaborated by electromagnetic brewing at 250 A. The used electrolytic medium are 3,5% NaCl and acidified 3,5% NaCl (pH 3). The results obtained from several techniques (Open circuit potential, Tafel curves, chronopotentiometry and electrochemical impedance spectrometry), indicate the existence of a heterogeneous structure in the silicon ingot.

I. Introduction

Global consumption of energy is constantly increasing. Most of it comes from fossil fuels (oil, natural gas, coal, etc.) whose massive use can lead to the depletion of these reserves and actually threatens the environment. This threat is manifested mainly through pollution and the global warming of the earth by the greenhouse effect.

The solar energy available on the Earth's surface is 36 Pet watts (1PW = 1015 Watts), while the wind energy resources are 72 TW (1TW = 1012 Watt), geothermal energy 9.7 TW, Use of human energy is 15TW [1-2].

The materials used initially by these photovoltaic cells were essentially inorganic. Today, the most commonly used material is still silicon, despite the increasingly stiff competition of cadmium tellurides, halides and other gallium arsenides [3 - 4].

The homogeneous and/or the heterogeneous structure of the silicon of the photovoltaic cells (PV) was studied in marine electrolytic medium with 3.5% NaCl and in a second electrolytic medium of the same chemical composition as the first but acidified to pH 3.

The existence of possible corrosion implies:

- Either the presence of a chemical heterogeneity in the form of segregation at grain boundaries or micro-precipitates in the grains.
- The presence of structural heterogeneity induced by cooling kinetics, especially during solidification (liquid-solid), will result in the presence of dislocations and twins [5].

Thus, the electrochemical experimental results allow us to pronounce if in practice the PV cells homogeneity was verified or no by these techniques.

II. Materials and methods

II.1. Sample Collection

The silicon samples, after preparation, were heated to 1200°C in an arc furnace. The inert atmosphere was controlled by a flow of argon. The samples were held for two hours at 1200°C.

The cooling was realized under the flow of argon gas that allows obtaining a temperature of 650°C after 4 hours. For the electrochemical study, we were interested in a half-ingot named Bb (figure 1). Samples Bb1, Bb2 and Bb3 cut under lubrication, of size (10 X 10 X 5) mm. The cylinder (liquid/solid) was cooled by the BRIDJMAN method. The working surface is 1 cm² [6].

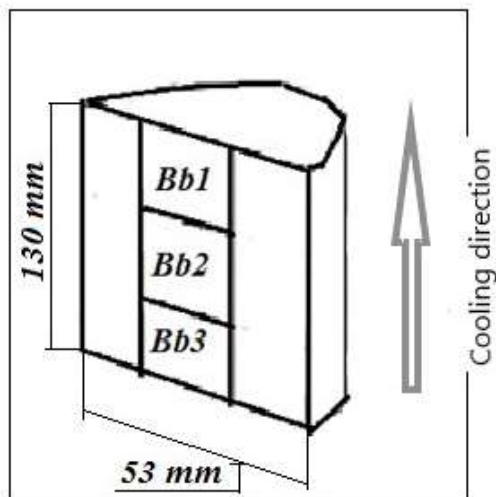


Figure 1. Schematic representation of a half-ingot and the position of the samples taken on the ingot Bb obtained with electromagnetic stirring at 250 A.

II.2. Electrolytes:

Two electrolytes were used: 3.5% NaCl representing the reconstitution of the sea water (about 35 g/l); and a 3.5% NaCl solution acidified with HCl at pH = 3.

II.3. Electrochemical techniques

The electrochemical tests are carried out using a three-electrode assembly, an electrochemical cell with double walls with a capacity of 500 ml. The potentials are given with respect to a saturated calomel SCE electrode. A graphite electrode was used as a counter electrode.

A volume of 200 ml of the electrolytic solution is filled into the electrochemical cell. The working electrode is placed in parallel with the counter electrode and the reference electrode is added so that the contact surface is very close to the working electrode.

The Tafel consists of applying to the working electrode potential from -300mV to + 300 mV around the corrosion potential and scanned at the rate of 0.016 mV.s⁻¹vs

II.4. Working electrodes

Before hand the sample has a surface area of 1 cm² which is glued to a metal plate using a conductive paste, initially polished with abrasive paper. The latter is welded to a conducting wire.

The assembly is coated with an insulating resin. Workings electrodes are Bb1, Bb2 and Bb3 taken from the ingot Bb and have been polished by an abrasive paper with different particle sizes (600, 1000 and 1200 grit) followed by polishing with a paste of alumina 6 to 1 μm.

III. Results and discussion

III.1. Open circuit potential

The open circuit potential is a parameter which indicates the thermodynamically tendency of a silicon to electrochemical oxidation in the electrolytic medium. After a period of immersion it stabilizes around a stationary value. This potential may vary with time because changes in the nature of the surface of the electrode that occur (oxidation, formation of the passive layer or immunity).

The open circuit potential is used as a criterion for the activity behaviour. Figure 2 shows the open circuit potential curves for the three samples Bb1-Bb3 immersed in 3,5% NaCl solution and in the acidified medium at pH 3.

- The heat treatment and its cooling rate bring a change in the electrochemical process. On the other hand, for the Bb1 electrode the nobility of the electrode was reduced since its potential went from -210 mV in NaCl medium to -710 mV in the same acidified medium.
- Also, the free corrosion potential of each electrode is different. It shows that the silicon structure is heterogeneous and that the chosen cooling has not permit to obtain the homogeneous mixture of the solid solution during its cooling. Figure 2a shows the evolution of the corrosion potential as a function of the immersion time of the three electrodes in a 3.5% NaCl solution. For the electrodes Bb2 and Bb3, the corrosion potential is shifted towards the more negative values compared to that of the electrode Bb1 where its potential becomes more noble. From these results, it appears clearly that the three electrodes, from the thermodynamic point of view, possess heterogeneous structures.

Figure 2b shows the evolution of the corrosion potential as a function of the immersion time in a solution formed of 3.5% NaCl acidified with HCl. The pH was adjusted to 3. The potential of these electrodes was modified, compared to the result obtained for the non-acidified NaCl solution, the order of the potential in this case follow the order from the positive value to the negative value (Bb3. □ Bb2 . □ Bb1). For the electrodes Bb3 and Bb1, the measured potential is characterized by instantaneous fluctuations. The characteristic values of the corrosion potential after 50 s of immersion are given in table 1.

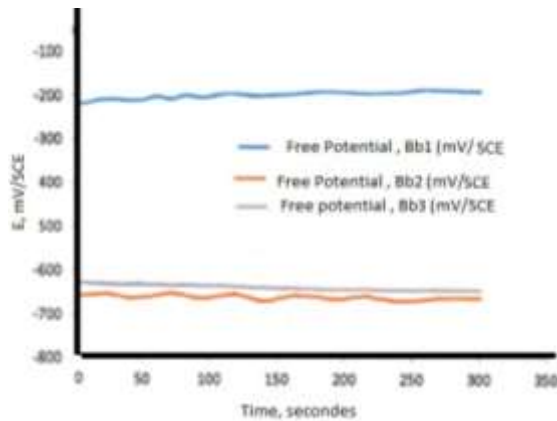


Figure 2a. Evolution of the free corrosion potential as versus time of immersion of the silicon working electrodes (Bb1, Bb2 and Bb3) in NaCl medium.

Table 1. Free open potential of 3 electrodes immersed in 3.5% NaCl and 3.5% NaCl acidified at pH = 3.

Electrolytique solution	Electrodes		
	Bb1	Bb2	Bb3
3,5%NaCl	-207	-670	-630
3,5%NaCl, pH=3	-710	-540	-482

The corrosion potential ($E_{corr.}$) of the Bb1 electrode is equal to -207 mV/ECS. This potential is the most noble than the electrodes Bb2 and Bb3. Thus, it is noted that the elaboration of the silicon gave a heterogeneous structure.

In the 3.5% NaCl medium acidified with HCl, we find that the displacement of the potential values is towards the less noble values. However, the change of the potential in both media is explained by the evolution of the pH towards the more positive values which is linked to the presence of the H^+ protons.

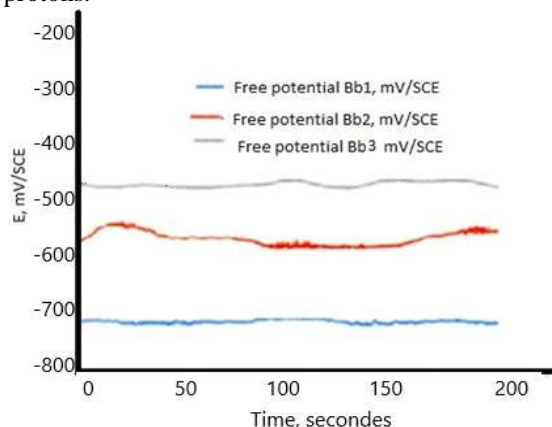


Figure 2b. Evolution of the free corrosion potential as a function of the time of immersion of the silicon working electrodes (Bb1, Bb2 and Bb3) in acidified NaCl medium.

III.2. Tafel Measurements

Tafel curves of silicon electrodes Bb1 – Bb3 in the two medium are shown in figures 3a and 3b. The electrochemical parameters from these curves are given in tables 1 and 2. It is noted that the dynamic corrosion potential of the electrodes Bb1 and Bb2 tends towards the more negative values compared to that of the electrode Bb3. The values in table 2 are respectively -748 V/ECS, -737 V/ECS, and -408 V/ECS for the electrodes Bb1 and Bb2 and Bb3. This table shows the evolution of the polarization resistance of the electrodes Bb1, Bb2 and Bb3 in the 3.5% NaCl medium.

The values of the polarization resistance of the electrodes Bb1, Bb2 and Bb3 are respectively 5.18, 1.48 and 61.23 $K.\Omega cm^2$. This shows that the electrode Bb3 is the most resistant with respect to the other two electrodes. The polarization resistance of the three electrodes medium in the 3.5% NaCl is oriented in the direction Bb1 → Bb2 → Bb3.

The diffusion of the electro-active species at the (electrode/solution) interface is small for the Bb1 electrode; this is due to the slowing down of the species which oxidize at the (electrode/solution) interface. For the electrodes Bb1 and Bb2, the value of the R_p is low, therefore the diffusion is stronger, which is due to the increase of the oxidizable electro-active species in the interface (electrode/solution).

It is noted that the corrosion rate of the electrode Bb3 is small compared with the electrodes Bb1 and Bb2. This is justified by the high electronegativity of the Bb3 electrode, compared to the other two electrodes. The electrode Bb3 is nobler than the electrodes Bb1 and Bb2, so it corrodes slowly.

Regarding the corrosion current of the electrodes Bb1, Bb2 and Bb3, (figure 3a), it is noted that it is higher with the electrode Bb1. It becomes smaller for the Bb3 electrode ($I_{corr(Bb1)} = 33,9 \mu A/cm^2$ and $I_{corr(Bb3)} = 0,66 \mu A/cm^2$) It is evident that the rate of corrosion is proportional to the corrosion current.

The characteristic values recorded from the potentiodynamic polarization curves of the electrodes Bb1, Bb2 and Bb3 are recorded in table 1 and 2.

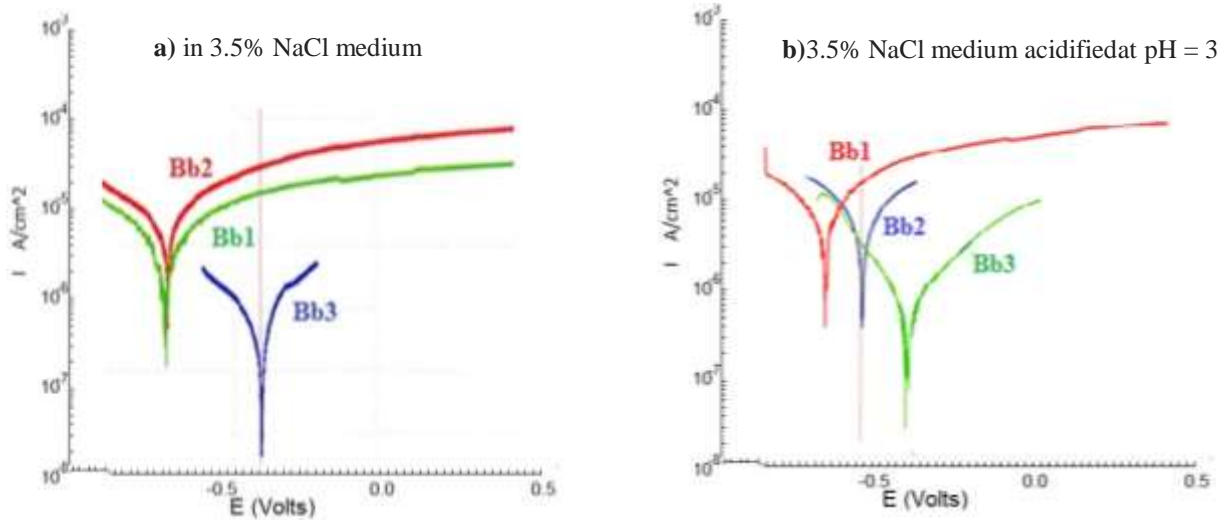


Figure 3. Tafel curves for the three electrodes Bb1, Bb2 and Bb3.

Table 1. Characteristic values of the polarization curves of electrodes Bb1, Bb2 and Bb3 in 3.5% NaCl.

Silicon electrodes	$E_i = 0$ (mV/ECS)	R_p (K.Ωcm ²)	I_{corr} (μA/cm ²)	β_a (mV)	β_b (mV)	V_{corr} (μA/an)
Bb1	-787	4,56	8,95	257,2	324,9	104,6
Bb2	-655	5,96	9,82	383,9	352,8	114,0
Bb3	-492	115,63	0,30	213,1	167,3	3,53

Table 2. Characteristic values of the polarization curves of electrodes Bb1, Bb2 and Bb3 in 3.5% NaCl medium acidified with HCl at pH = 3.

Silicon electrodes	$E_i = 0$ mV/ECS	R_p K.Ωcm ²	I_{corr} , (μA/cm ²)	β_a (mV)	β_c (mV)	V_{corr} (μA/an)
Bb1	-737	1,48	33,9	415	565	397
Bb2	-748	5,18	9,16	294	272	107
Bb3	-408	61,23	0,66	206	270	7,80

It is noted that the dynamic corrosion potential of the three electrodes oriented respectively in the direction Bb1 → Bb2 → Bb3. The potential of the electrodes Bb1 and Bb2 tends towards the more negative values comparing to the electrode Bb3. From these potential values, it is found that the electrode Bb3 is nobler than electrodes Bb1 and Bb2. The classification of the electro negativity of the three electrodes is as follow:

Bb1. → Bb2 .→ Bb3 for electrodes in NaCl medium and

Bb2 .→ Bb1 .→ Bb3 in the acidified NaCl medium

From Table 2, polarization resistances are 4.56, 5.96 and 115.63 K.Ohms*cm² for electrodes Bb1, Bb2, Bb3 respectively. From these results, it can be seen that the Bb3 electrode is the most resistant comparing to Bb1 and Bb2 electrodes.

It can be seen from the results given in Tables 1 and 2 that the bias resistance of the electrodes Bb1, Bb2 and Bb3 is different for the two media.

From these values, the anodic constant (β_a), of the electrode Bb1, Bb2 and Bb3 are respectively 257.2; 383.9 and 213.1 mV. It can be seen that for the Bb2

electrode, the diffusion of the electro-active species at the interface (electrode/solution) was smaller; this is due to the increase of the electro-active species near these interface.

III.3. Chronopotentiometry:

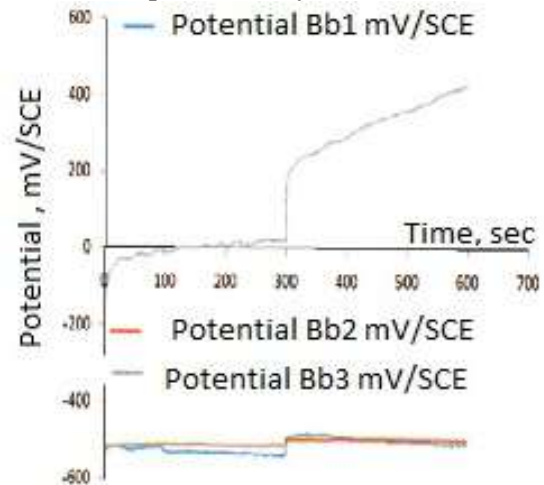
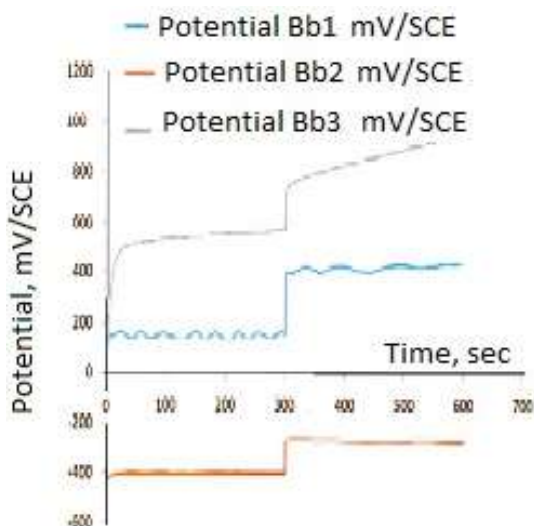


Figure 4a. Chronopotentiometric curves of the three silicon electrodes in the 3.5% NaCl medium



The three electrodes were galvanically activated in two steps. The imposed current values are illustrated in table 3.

Figure 4b. Chronopotentiometric curves of the three silicon electrodes in the 3.5% NaCl medium in acidic medium pH 3.

Table 3. Imposed current and corresponding potentials

Electrodes	3.5% NaCl medium			3.5% NaCl medium pH 3		
	Bb1	Bb2	Bb3	Bb1	Bb2	Bb3
Imposed current (mA)	0,08 et 0,1	0,66 et 0,9	0,001 et 0,009	0,037 et 0,05	0,033 et 0,05	0,002 et 0,01
Corresponding potential (mV)	-587,3 et -533,75	-717,1 et -509,25	-365,5 et -20,88	-665,4 et -160,38	-507,7 et -400,43	-244,9 et -570,13

The activation of the electrodes to the oxidation currents indicated in table 3 shows through the curves illustrated in figure 4a that the electrode Bb3 is the most reactive, since the current jump passing from 0.001 to 0.009 mA after 300 seconds. This increase shows the appearance of a new resistance caused by the modification of the active surface of the electrode. During a test period of 300 seconds, the overvoltage of the Bb3 electrode decreased from -365.5 to -20.88 mV/ECS. For the Bb1 electrode, the potential has increased from -587.3 to -533.75 and that of the Bb2 electrode has changed from -717.1 to -509.25 mV/ECS. The potential of these last two electrodes (Bb1 and Bb2) remained relatively stable.

The imposed current values for the three silicon electrodes in 3.5% NaCl medium acidified with HCl at pH = 3 are summarized in Table 3. The activation of the electrodes in the acidified medium to the oxidation currents indicated in Table 3 shows through the curves illustrated in figure 3b that the electrode Bb3 is the most reactive because the current jumps from 0.002 to 0,01 mA after 300 seconds. The increase of current shows the appearance of a new activity caused by the

modification of the active surface of the electrode. During a test period of 300 seconds, the overvoltage of the Bb3 electrode shift from 244.9 to 570.13 mV/ECS. For the Bb1 electrode, the potential has moved from -665.4 to -160.38 mV/ECS and the current of the Bb2 electrode was evolved from -507.7 to -400.43 mV/ECS. The potential of these last two electrodes (Bb1 and Bb2) remained relatively stable with respect to Bb3.

III.4. Electrochemical Impedance Spectrometry (SIE) measurements

In order to confirm the obtained results by potentiodynamic polarization measurements and gather some information about the segregation mechanism of silicon under heating and cooling, the electrochemical impedance spectroscopy was also used. The advantage of this method is that both the polarization resistance values and the double layer capacitance values can be obtained in the same measurement. Figures 5 and 7 show the Nyquist plots of silicon in aerated 3,5% NaCl, and 3,5% NaCl-HCl (pH = 3) respectively. The

impedance diagrams do not present a perfect semicircle, generally attributed to the frequency dispersion [16] due to the surface heterogeneity. This heterogeneity results from the roughness, impurities, dislocations, the adsorption chemical species and the formation of porous layers on the surface of active electrode [18, 19].

In the 3,5% NaCl medium, the impedance Nyquist diagrams present one capacitive loop at higher frequency and another flattened semicircle at low frequency (Figure 5). In the neutral electrolyte (3,5% NaCl), the complex plane plots reveal the presence of two capacitive loops. The first at high frequencies with low capacitive values was attributed to the adsorbed water molecules on the silicon surface. The second at low frequencies correspond to the polarization resistance that it was attributed to the charge transfer.

Tables 4 and 5 gives the values of the charge transfer resistance R_t , double-layer capacitance C_d obtained from the EIS plots. It can be seen that the heat treatment of silicon and its cooling give a heterogeneous structures. EIS results confirm those obtained by potentiodynamic polarization curves. The obtained impedance data has been interpreted using the equivalent electrical circuit of Figure 6, where C_f and R_f present the adsorbed water parameters, the C_d is the double layer capacitance, and R_t is the charge transfer resistance.

Figure 7 illustrates the set of impedance diagrams of Bb1, Bb2 and Bb3 electrodes in NaCl medium acidified in HCl (pH = 3)

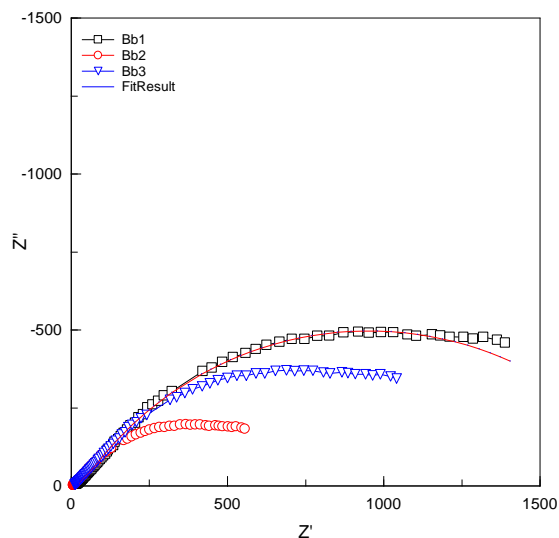


Figure 5. Nyquist plots of silicon electrodes in 3,5% NaCl at room temperature.

The electrochemical parameters extracted from Nyquist spectrums are given in Tables 4 and 5.

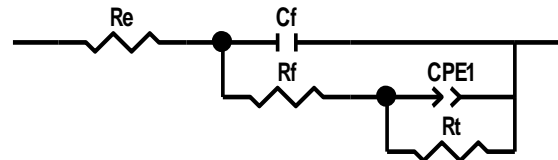


Figure 6. Electric equivalent circuit, NaCl medium

Table 4. Electrochemical Impedance spectroscopy parameters for silicon in 3,5% NaCl.

Elements	Working Electrodes		
	Bb1	Bb2	Bb3
$R_e, \Omega \cdot \text{cm}^2$	22,91	6,37	8,82
$C_f, \text{F/cm}$	$5,03 \cdot 10^{-7}$	$6,75 \cdot 10^{-7}$	$2,04 \cdot 10^{-7}$
$R_f, \Omega \cdot \text{cm}^2$	33,08	8,36	0,4
CPE-T, F/cm	$5,34 \cdot 10^{-5}$	$14,10 \cdot 10^{-5}$	$11,70 \cdot 10^{-5}$
CPE-P	0,62	0,60	0,0021
R_t	1832	770,10	14,94

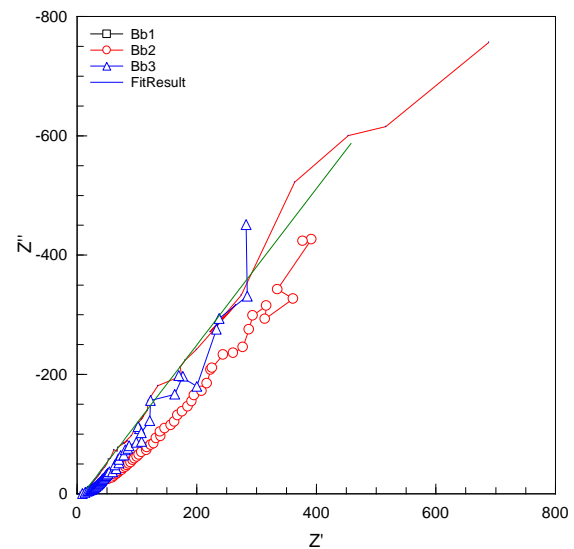


Figure 7. Nyquist plots of silicon electrodes in 3,5% NaCl- HCl at room temperature.

Table 5. Electrochemical Impedance spectroscopy parameters for silicon in 3,5% NaCl acidified at pH 3.

Components /Samples	Bb1	Bb2	Bb3
R_s	10,22	35,77	19,29
CPE-T	$6,51 \cdot 10^{-5}$	$3,77 \cdot 10^{-5}$	$8,54 \cdot 10^{-5}$
CPE-P	0,585	0,501	0,550

We used the Zview software to estimate the components of the interface. Using this software, the resistances and capacities of the circuit were calculated. The electrical circuit of the fitting interface (electrode/solution) consists of the elements R_e , C_f , R_f , CPE and R_t .

The impedance diagram in the representation of Nyquist of the electrode Bb1 is formed by a capacitive arc of a circle. The resistance of the

solution is located at the intersection of the semicircle of the impedance at high frequencies with the real axis of impedance. At low frequencies, the semicircle intersects the axis of the real axis and the element of the circuit represents the resistance of adsorbed water molecules R_f and the resistance of the solution R_s , because the capacitive semi-circle is flattened and the capacitance of the circuit has been replaced by a CPE which takes into consideration a degree of flattening. The results are shown in Table 4.

IV. Conclusion

The electrochemical characterization in two media allows us to know the effect of the heat treatments and its cooling on the structural state of silicon.

For this purpose, the electrochemical study was carried out on the 3 samples Bb1, Bb2 and Bb3 taken from the ingot Bb.

The obtained results confirm that the two electrodes cut from the two ends "top and bottom of the ingot Bb" and from the middle of the ingot «Bb2» have more negative potential values compared to that of the sample taken from the middle «Bb3» which has more noble values of potential. From these results, it has been found that the three silicon electrodes have heterogeneous structures.

According to the potentiodynamic polarization curves (Tafel), it was found that the electronegativity of the 3 electrodes is different and it is classed in the following direction Bb1 → Bb2 → Bb3.

The electro-active species at the electrode/solution interface differ from one electrode to another by diffusion kinetics that vary from one electrode to another.

The chronopotentiometric curves show the difference in the reactivity of the surface of the three silicon electrodes.

According to the electrochemical impedance spectrometry it reveals that the electrical parameters of the circuits obtained are not identical. During the solidification carried out, chemical or structural segregation or both was observed.

In general, the heat treatment and cooling of the silicon gives a heterogeneous structure. The present study has shown the validity of electrochemical techniques in the characterization of the homogeneity and / or heterogeneity of the structure of silicon.

V. References

1. Tao, C.S.; Jiang, J.; Tao, M. Natural resource limitations to terawatt-scale solar cells. *Solar Energy Materials and Solar Cells* 95 (2011) 3176.
2. Shah, A.V.; Platz, R.; Keppner, Thin H. film silicon solar cells: a review and selected trends. *Solar Energy Materials and Solar Cells* 38 (1995) 501.
3. Elwell, D.; Feigelson, R.S. Electrodeposition of solar silicon. *Solar Energy Materials* 6 (1982) 123.
4. De Mattei, R.C.; Elwell, D.; Feigelson, R.S. Electrodeposition of silicon at temperatures above its melting point. *Journal of the Electrochemical Society* 128 (1981) 1712.
5. Olson, J.M.; Carleton, K.L. A semipermeable anode for silicon electrorefining. *Journal of the Electrochemical Society* 128 (1981) 2698.
6. Kliemt, K.; Krellner, C. Crystal growth by Bridgman and Czochralski method of the ferromagnetic quantum critical material YbNi₄P₂. *Journal of Crystal Growth*, June 20 (2016).
7. Sharma, I.G.; Mukherjee, T.K. A study on purification of metallurgical grade silicon by molten salt electrorefining. *Metallurgical and Materials Transactions B* 17 (1986) 395.
8. Jacobson, A. C. Evaluation of global wind power. *Geophysical research*, vol. D12110 (2005) p. 110
9. ERGE T, S. F. Photovoltaic in buildings, a design handbook for architects and engineers», Paris, France: *International energy agency*(1996)
10. Bailly, L. Cellules photovoltaïques organiques souples à grande surface. Thèse de doctorat. Université BORDEAUX I. *Septembre 2010*.
11. Astier, S. Conversion photovoltaïque de la cellule aux systèmes, *Techniques de l'ingénieur. D 3936 (2008)*.
12. Bard, A. J. Ed. Encyclopedia of Electrochemistry of the Elements. *Dekker, M. 270 Madison Avenue NEW YORK NY 10016, Volume IX-A, 612 p, USA (1982)*
13. Hine, F.; Electrode Processes and Electrochemical Engineering (Réactions aux électrodes et Génie électrochimique). *Plenum Press, 233 Spring Street NEW YORK NY 10013, USA (1985) 410 p.*
14. Besson, J. - Précis de Thermodynamique & Cinétique électrochimiques. *Ellipses-Edition Marketing. 75015 PARIS. S. (1984) 446 p*
15. Bommersbach, P.; Alemany-Dumont, C.; Millet, J.P.; Normand, B. Hydrodynamic effect on the behaviour of a corrosion inhibitor film: Characterization by electrochemical impedance spectroscopy. *Electrochimica Acta*. 51, No.19 (2006) 4011-4018.
16. Macedo, M.C.S.S.; Margarit, I.C.P.; Fragata, F.L.; Jorcin, J.B. Contribution to a better understanding of different behaviour patterns observed with organic coatings evaluated by electrochemical impedance spectroscopy. *Corroion. Sciences*. 51(6)(2009) 1322 – 1327.
17. Gupta, G.K.; Garg, A.; Dixit, A. Electrical and impedance spectroscopy analysis of sol-gel derived spin coated Cu₂ZnSnS₄ solar cell. *Journal of Applied Physics*. 123 (2018) 013101
18. Fabregat-Santiago, F.; Garcia-Belmonte, G.; Mora-Sero, I.; Bisquert, J. Characterization of nanostructured hybrid and organic solar cells by impedance spectroscopy. *Physical Chemistry Chemical Physics*. 13 (2011) 9083–9118.
19. Shibayama, N.; Zhang, Y.; Satake, T.; Sugiyama, M. Modelling of an equivalent circuit for Cu₂ZnSnS₄-and Cu₂ZnSnSe₄ based thin film solar cells. *Royal Society of Chemistry Advances*. 7 (2017)25347–25352.

Please cite this Article as:

Salhi N., Salhi E., Bounoughaz M., Electrochemical characterization of semiconductor photovoltaic silicon, *Algerian J. Env. Sc. Technology*, **8:4 (2022) 2813-2820**